JOURNAL

of

STEEL CASTINGS RESEARCH

CONTENTS

Thermal Conductivity of Rammed Sand Mixtures 1

A Study of Some Foundry Variables Affecting the Occurrence of Visible Nonmetallic Surface Defects in Steel Castings 7

Abstracts of Fundamental Papers on Steel Castings Research 14

Index to Journal, Numbers 1-23, incl. 15

STEEL FOUNDERS' SOCIETY OF AMERICA

NUMBER 23 OCTOBER, 1961

JOURNAL OF STEEL CASTINGS RESEARCH

Number 23 October, 1961

TECHNICAL RESEARCH COMMITTEE, SFSA

V. E. ZANG, Unitcast Corporation, Chairman

F. H. ALLISON, JR., Foundry & Mill Machinery Division, Blaw Knox Company

H. H. BLOSJO, Malleable Iron Fittings Company

W. K. BOCK, National Castings Company

A. P. GUIDI, Texas Foundries, Inc.

G. F. HAISLUP, Electric Steel Castings Company

J. M. HATHAWAY, The Massillon Steel Casting Company

C. B. JENNI, General Steel Industries, Inc.

CHARLES LOCKE, Crucible Steel Casting Company

PHILIP McCAFFERY, General Metals Corporation

C. E. STULL, The Pelton Steel Casting Company

R. O. TIBBALS, American Steel Foundries

DIRECTOR OF RESEARCH AND JOURNAL EDITOR
CHARLES W. BRIGGS

EDITORIAL STAFF

R. A. WILLEY,
Assistant Technical
and Research Director

DENNIS C. HARSCH,
Assistant to the Technical
and Research Director

© by Steel Founders' Society of America, 1961

606 Terminal Tower Cleveland 13, Ohio

THE CIRCULATION OF THE JOURNAL IS RESTRICTED TO MEMBERS OF THE SOCIETY AND OTHERS AS AUTHORIZED BY THE BOARD OF DIRECTORS

THERMAL CONDUCTIVITY OF RAMMED SAND MIXTURES

by

R. J. Mittendorf* and D. C. Williams**

The thermal conductivity of rammed sand mixtures has been reported by Paschkis[3][4], Brandt, Bishop and Pellini[5][6][7] and Lucks[8] when the sand was in the dry condition. Adams and Taylor[9] give values for the green sand condition. Our literature search did not reveal any data relative to the effect upon thermal conductivity of compositional changes within the sand mixture.

It has been assumed that the thermal conductivity of green sand is greater than that of dry sand and that such dry sand will serve as a thermal block. Therefore, it may be asked of what value is a knowledge of the thermal conductivity of green sand. One factor controlling heat flow in a sand mass is the thermal gradient within the mass. The thermal gradient within dry sand can be up to seventeen times the gradient in green sand. However, the thermal conductivity of green sand may approach a value five times that of dry sand. Where commercial alloys are involved, the maximum thermal gradient in green sand will be the temperature difference between the boiling point for water and the ambient mold temperature.

The value which is designated the coefficient of thermal conductivity for green sand masses is not a true value in the most rigorous sense. For heat to flow through a green sand mass there must be a temperature gradient, and the water in the green sand mass will be subject to a pressure gradient. This pressure gradient will tend to cause water to flow to a site of lower temperature, thus transferring some heat by convection. Under the test conditions reported herein, the heat transfer by convection is negligible, and therefore the values found for the coefficient of thermal conductivity closely approach true values. (In the establishment of the water envelope around a casting, the pressure gradient in green sand may be a considerable contributing factor.)

The theory used in these studies is presented by Fitch[10] and Schuhmann[11]. The basic equations are

$$(a)\quad Q = C_p m dt \ .$$

and

$$(b)\quad q = -k_{av}\ \frac{2\pi l \triangle t}{2.3 \log \frac{r_2}{r_1}}$$

It needs only to be stated here that in the equation

$$k = \text{slope}\ \left(\frac{\log N}{r}\right) \times \frac{2.3\ C_p m d\ l}{A}$$

$\frac{2.3\ C_p m d\ l}{A}$ is a constant for any given apparatus and for the particular equipment used in this investigation the value is .397.

APPARATUS

The cylindrically shaped test apparatus is presented schematically in Figure 1. The source of heat is a converted fruit juice tin can (a) into which hot water is introduced and brought to boiling temperature by an immersion type electrical heating unit of 1300 watts. The cold face is a cylindrical brass sheet indicated as (b). The compacted cylinder of sand is indicated by (d). The entire assembly is encased in styrofoam (c) insulating materials. The iron-constantan thermocouple (e) was so attached to the cylindrical brass sheet that at least six inches of each lead wire, adjacent to the bead, was in an isothermal plane with the bead. A moisture teller was used to ascertain the moisture content of the mixtures tested.

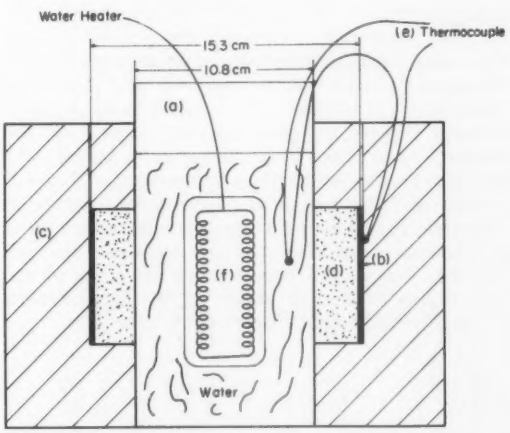

Figure 1—Representation of test apparatus to determine thermal conductivity (K) of green sand mixtures,

(a) = cylinder to contain water at 212°F
(b) = brass cylinder - cold fore
(c) = styrofoam insulation
(d) = cylinder of sand compact
(e) = differential thermocouple
(f) = 1400 watt immersion type heater

* Student in Metallurgical Engineering at The Ohio State University, present address.

** Associate Professor, Department of Metallurgical Engineering, The Ohio State University, Columbus, Ohio.

PROCEDURE

The sand mixtures were prepared using a Paul O. Abbe ribbon flight mixer (see Figure 8[12]). All sand mixtures were rammed to an average density of 90 lbs./ft.^{3}. After compaction of the test specimen boiling water was introduced into the heat source, central cylinder, and the immersion heater was put in place and turned on. No differential thermocouple readings were taken for the first few minutes as a short period of time was required for the heater to restore the water temperature to the boiling point. Potentiometric readings were recorded, beginning when the temperature level of the cold face began to rise, and readings were concluded when the sand adjacent to the hot face (central cylinder) indicated evidence of drying out.

RESULTS

The equipment used does not permit the evaluation of thermal conductivity of mixtures composed of sand grains and water. Any slight reduction in water content causes a reduction in the bulking action and a minute but perceptible reduction in contact area about the hot face. To obtain the thermal conductivity of sand water mixtures would require equipment alterations. To overcome the effect of bulking loss it was found that it was sufficient to add 1 percent of western bentonite to the mixtures.

Figure 2 schematically presents the relation between log N and time, where N is the temperature difference between the two thermocouple junctions. Within time period (1) the water temperature is being restored to 100 degrees C. During time period (2) the temperature difference between the hot and cold faces does not change and a thermal gradient is being established within the rammed sand mass. The duration of time period (2) varied from one to three minutes depending upon moisture content of the mixture under test. It is during time period (3) that the thermal conductivity is measured, and it will be noticed that the slope of the line does not change. This time period covers a span of time varying from five to fifteen minutes depending upon the moisture content. Period (4) begins when the slope of the line begins to deviate indicating the formation of dry sand immediately adjacent to the hot face.

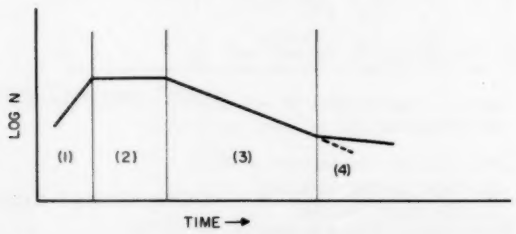

Figure 2—Schematic representation of relationship between log N and time within the test equipment.

The initial investigations involved determinations using dry sand compacts to check out the equipment and to compare results with data found in handbooks. The quartz sands were supplied by the Central Silica Company of Zanesville, Ohio, in two grades, coarse (A.F.S. Fineness No. 60) and fine (A.F.S. Fineness No. 110). These sands were permitted to set for six months under ambient temperature conditions of the laboratory before testing and were not oven dried before testing. Separate tests revealed that the moisture content (at 212 degrees F) for the two grades of sand was 0.2 percent. The K values found were 0.9 and 0.95 x 10^{-3} cal./sec. cm. °C respectively for the coarse and fine quartz sands, where K is the coefficient of thermal conductivity of green sand. The handbook yields a value of K = 0.93 cal./sec. cm. °C, and therefore it was accepted that the equipment was functioning adequately.

The heat dissipated into the mold during the solidification of an alloy and subsequent cooling of the solid alloy subjects the quartz grains to a heat treatment. To simulate a rather severe heat treatment five pounds of each size of quartz grains were heated in a furnace at 1650 degrees F for 72 hours and

TABLE I

K values for sand-water 1% bentonite mixtures, coarse and fine sands as the moisture content varies. Also the ratio between K (moist) and k (dry), K_m/K_d

Moisture		K x 10^{-3} Cal. sec. cm. °C		
Wt. % (M_w)	Vol. % (M_v)	Coarse	Fine	K_m/K_d
0.5	0.80	1.50		1.67
0.6	0.95	1.35		1.50
0.7	1.10	1.95		2.16
0.7	1.10	1.95		2.16
0.9	1.45	1.80		2.00
1.2	1.90	1.70		1.89
1.3	2.05		2.00	2.22
1.3	2.05		2.00	2.22
1.4	2.20	2.00		2.22
1.7	2.70	2.20		2.47
2.4	3.80	2.50		2.78
2.6	4.15	3.20		3.55
2.6	4.15	3.10		3.44
2.7	4.30		3.05	3.40
2.8	4.50	3.60		4.00
3.5	5.60	4.50		5.00
3.5	5.60	3.90		4.34
4.1	6.60		3.60	4.00
4.7	7.55	4.10		4.56
4.7	7.55	4.00		4.45
5.8	9.30		3.80	4.22
6.3	10.10	5.60		6.24
7.1	11.40		3.80	4.22
9.0	14.45		4.70	5.22

oven cooled to room temperature. The K values found were 0.85 and 1.0 x 10^{-3} cal./sec. cm. °C for the coarse and fine sands respectively. The above values were obtained using compacts not oven dried, and the moisture contents of the heat treated quartz sands were 0.1 percent and 0.3 percent respectively for the coarse and fine sands. The spread of K values between the two sizes of grains in the heat treated condition may be important for those interested in the durability of sand mixtures.

The experimentally determined values of K for the various mixtures tested are given in Tables I and II

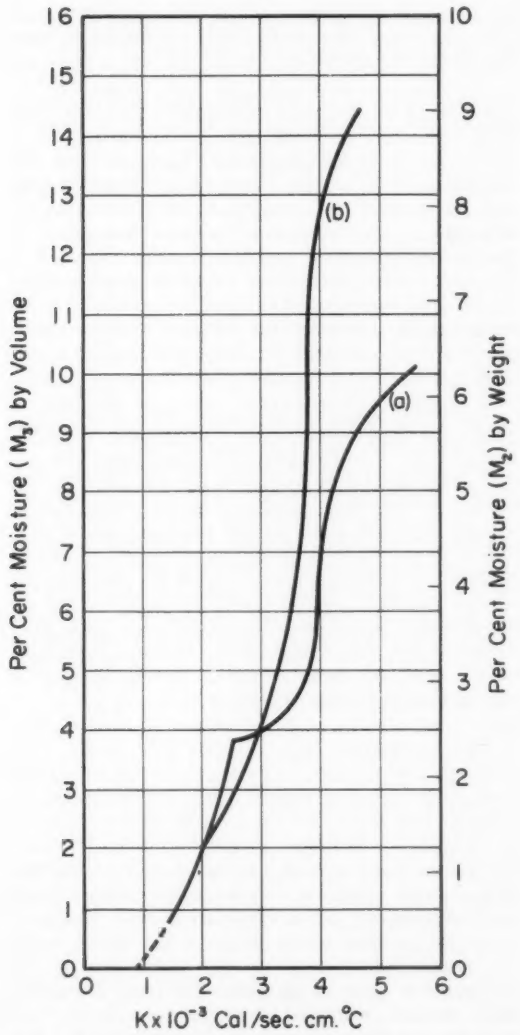

Figure 3—Relationship between coefficient of thermal conductivity for sand mixtures and moisture content. Sand mixture (a) coarse sand—1% western bentonite and sand mixture (b) fine sand 1% western bentonite.

as K varied with moisture content. The values in Table I are plotted in Figure 3 while the values of Table II are plotted in Figure 4. The general shape of all the curves indicates that the value of K increases with moisture content (M_3) up to 6 percent, then remains constant as the moisture varies, until at some higher level K may again increase with moisture. Additional testing will be required to establish the variation of K with moisture content (M_3) above 12 percent.

From Figure 3 for the coarse and fine sand with 1 percent western bentonite, the asymptotic value for K is approximately 4.0 x 10^{-3}. For mixtures containing corn flour, sea coal, and increased amount of bentonite, the asymptotic value of K approaches 3.0 x 10^{-3}, or a reduction of 25 percent in the value of K.

Expressing the moisture content as M_2 or M_3 is the

TABLE II—K values for green sand mixtures (coarse sand) as the moisture content varies

Moisture		K x 10^{-3} Cal.	
Wt. % (M_2)	Vol. % (M_3)	sec. cm. °C	K_m/K_d
4% Western Bentonite			
1.7	2.70	1.55	1.72
2.8	4.45	2.70	3.00
2.8	4.45	2.50	2.78
3.6	5.75	2.20	2.44
5.1	8.15	3.20	3.56
5.1	8.15	3.10	3.44
6.8	10.90	3.10	3.44
9.4	15.05	4.10	4.55
1% Corn Flour—1% Western Bentonite			
1.6	2.55	1.55	1.72
2.4	3.85	2.10	2.33
2.6	4.15	2.10	2.33
4.5	7.20	2.60	2.89
4.5	7.20	2.70	3.00
4.5	7.20	2.40	2.66
4.6	7.40	2.30	2.56
6.6	10.60	3.70	4.11
8.2	13.15	3.30	3.67
4% Sea Coal—1% Western Bentonite			
0.5	0.80	1.00	1.11
1.2	1.90	1.70	1.89
1.8	2.85	1.90	2.11
1.9	3.00	2.20	2.44
2.0	3.20	2.15	2.38
2.1	3.40	2.20	2.44
2.7	4.30	2.45	2.85
3.4	5.45	3.20	3.56
3.6	5.75	2.80	3.11
3.8	6.05	2.70	3.00
5.1	8.15	3.00	3.33
6.4	10.25	3.25	3.61
7.8	12.50	3.40	3.78

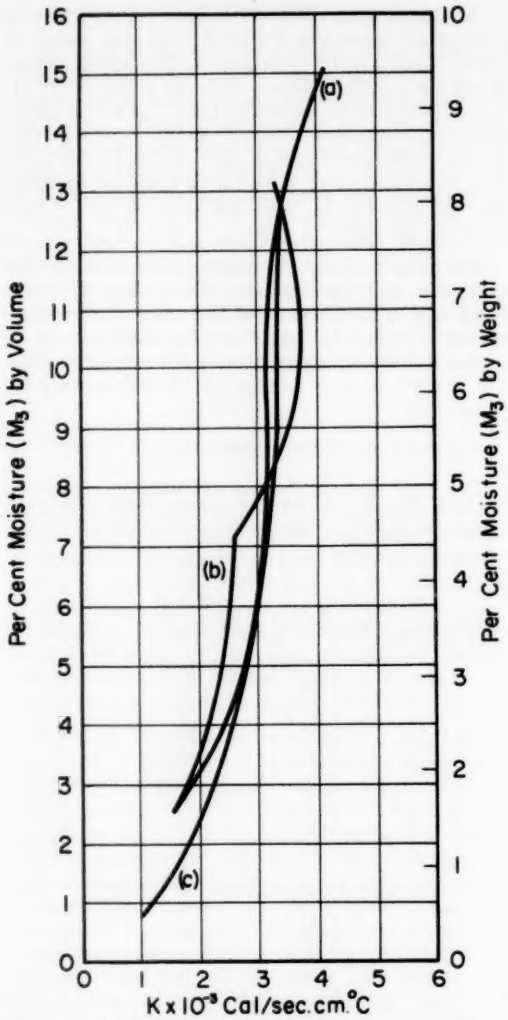

Figure 4—Relationship between coefficient of thermal conductivity for sand mixtures (coarse sand) and moisture content. Mixture (a) - 4% western bentonite. Mixture (b) - 1% corn flour and 1% western bentonite. Mixture (c) - 4% sea coal and 1% western bentonite.

designation used by Paschkis[13]. Figure 5 shows the relationship between moisture content by weight (M_2) and moisture content by volume (M_3) when the density of the rammed green masses varies between 80 and 100 lbs./ft.^{3}.

DISCUSSION

One of the reasons for this investigation to determine the coefficient of thermal conductivity of green sand mixtures was to learn whether the coefficient (K) was related to any particular component of sand mixture. During this discussion the units for K will be considered as cal./sec. cm. °C and

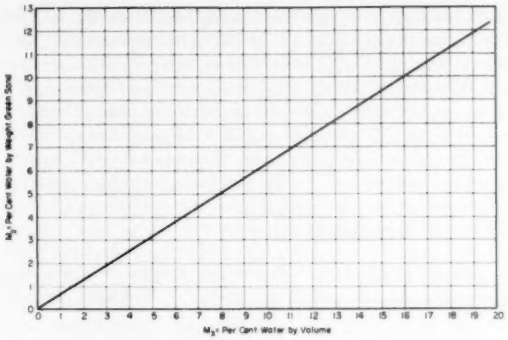

Figure 5—Relationship between moisture content, of rammed green sand masses, expressed by weight and by volume when the density varies between 80 and 100 lbs/ft^3.

expressed in terms of 10^{-3}. Hereinafter only the actual numerical values related to the above will be given.

Quartz, the major component of the mixtures, has a K value of 30 parallel to the main crystallographic axis and a value of 16 normal to the main axis. Assuming in a sand mixture the random orientation of the quartz grains one might expect that the average K value due to quartz alone would approach a value of 23. The determined values of K were found to be separated too far from this value so that it appears that thermal conductivity in green sand mixtures does not involve the quartz grains.

It will be recalled that the dry sand subjected to prolonged heat treatment at 1700 degrees F had K values close to those provided in handbooks and that the moisture content of such sands were 0.3 percent or below. The heat treatment was not sufficient to change the sand grain surface from the silanol condition to the siloxane condition. ("Silanol" refers to a surface condition of the sand grain wherein one or two hydroxyl groups (OH) are absorbed on the amorphous silica surface of the sand grain. "Siloxane" refers to the condition wherein, through heat treatment, water has been removed, leaving oxygen on the surface as pictured below.)

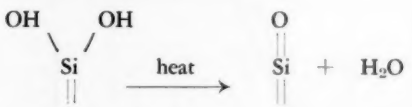

It is considered that the K value of 0.85 for the heat treated coarse sand (whose moisture content was 0.1 percent) is more dependent upon that moisture content than to the silica of the quartz grain. To obtain the K value for oven dried sand at 212 degrees F it appears necessary that after drying the sand should be cooled to room temperature and tested at room temperature in a completely moisture free atmosphere.

Water has a K value of 1.4 and most of the determined K values exceeded this value so that it

appears that the thermal conductivity of green sand mixtures is not related to stoichiometric water.

Williams[14] has proposed that the bonding mechanism in foundry sands depends upon the establishment of a layer of silica gel around sand grains and that the source of the silica for gel formation is the H.S. silica layer upon each sand grain. (The "H.S. silica layer" refers to the high soluble silica layer on quartz grains, sometimes called the "disturbed layer." This layer is present as amorphous SiO_2 about .03 microns thick.[14]) This layer of silica gel has been variously described as "rigid water," "ice film," "immobilized water" and "non-stoichiometric water."

The K values for ice reported in the literature are 2.2, 3.9, 5.0, 5.25 and 5.35. It will be noticed that these values bracket most of the K values determined for the green sand mixtures tested. There are at least three crystallographic forms of ice known (described as ice I, ice II and ice III), however it could not be learned whether any of the K values for ice were related to a particular ice form. From Figures 3 and 4 it will be seen that up to 6 percent moisture by volume (4 percent by weight), the K value increases with moisture content. It is suggested that up to 6 percent moisture, the water in the silica gel has a crystallographic structure corresponding to one of the ice forms. It may be that within this moisture range there is a transition from one ice form to another. This might be possible, for between 6 and 12 percent moisture by volume there is very little change in the K value, suggesting that another of the ice forms has come into existence. Above about 12 percent moisture by volume, the K value changes with moisture, suggesting a change to still another of the ice forms. Even though there is considerable uncertainty regarding a relation between K values and ice forms it does appear that the thermal conductivity of green sand mixtures is related more to the condition of non-stoichiometric water surrounding the sand grains than to other components of green sand mixtures.

All the curves of Figures 3 and 4 become asymptotic at about 6 percent moisture content (M_3). Figure 6 shows that for three sand mixtures using fine sand, the green compressive strength also becomes asymptotic at the same moisture content. The green strength curves were reported previously by Williams,[15] and the mixing procedure was given at that time. The equipment used in determining the K values was not adequate to develop data above a moisture content (M_3) of about 14 percent. This could be done if a heater of more than 1300 watts was secured. From the relationships in Figure 6, it is suggested that further evidence be presented to show that the green compressive strength depends upon the characteristics of the non-stoichiometric water in the film of gel surrounding the sand grains.

Paschkis[16], in his Figure 12, reports on the results of Tanasawa,[17] who studied the thermal conductivity of green molding sands. The results of study at Ohio State show a very good correlation with those presented by the two authors mentioned immediately above. The ratio K_m/K_d, where $K_d = 0.9 \times 10^{-3}$, for each test condition will be found in Tables I and II, and is plotted in Figure 7. In general, it will be seen that the curves for the sand mixtures tested have the same general shape as that found by Tanasawa.

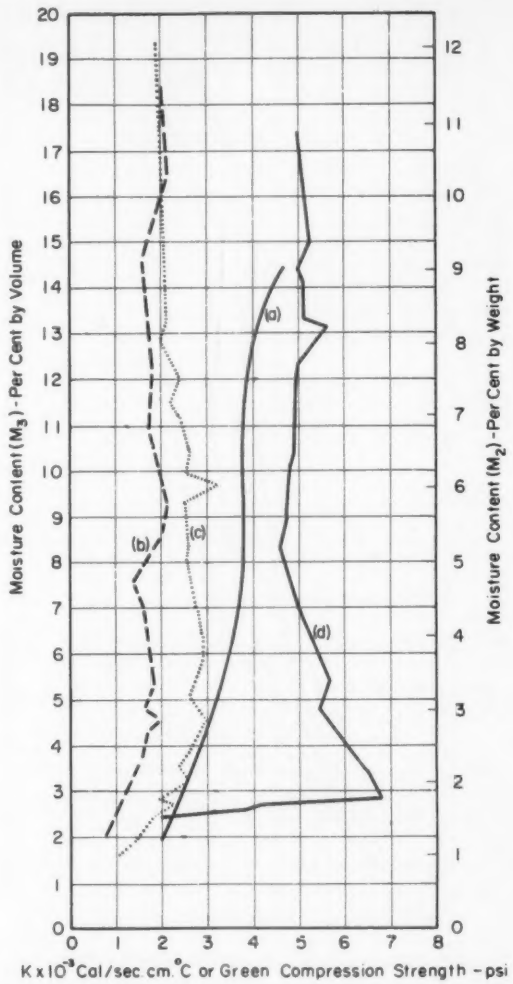
Moisture Content (M_3) - Per Cent by Volume
Moisture Content (M_2) - Per Cent by Weight
K x 10^{-3} Cal/sec cm °C or Green Compression Strength - psi
(a)
(b)
(c)
(d)

Figure 6—Relationships between the coefficient of thermal conductivity (K) and moisture content, curve (a); and green compressive strength and moisture content, curves (b), (c), and (d).

(a) fine sand - 1% western bentonite
(b) fine sand - water
(c) fine sand - 2.5% western bentonite
(d) fine sand - 5% western bentonite

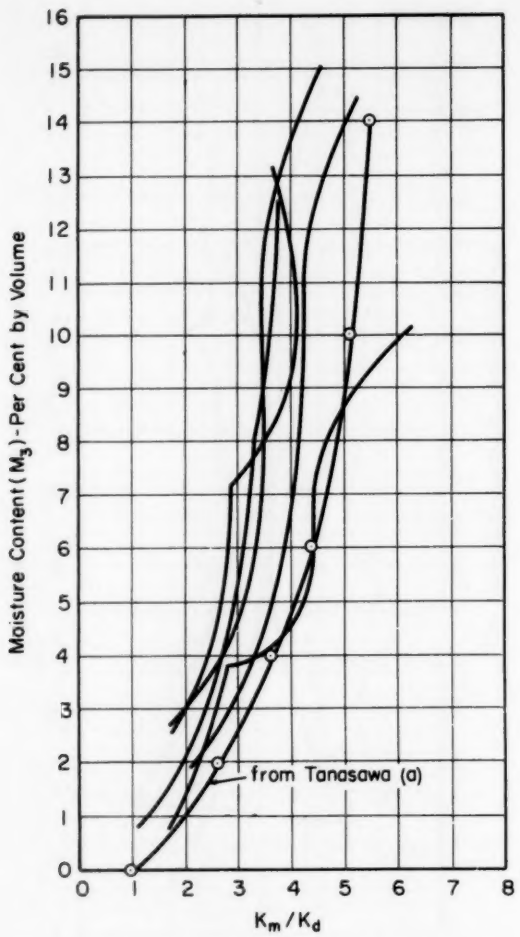

Figure 7—Relationship between moisture content of sand mixtures and K_m/K_d. Curve (a) from Tarasawa and the other curves from Tables I and II.

CONCLUSION

The coefficient of thermal conductivity (K) of green sand mixtures was found to vary with the moisture content, content of certain bonding materials, and one additive. The K values appear to be more closely related to the non-stoichiometric condition of the water (or "ice film") within the silica gel surrounding the sand grains than to the other components of the sand mixture. It is suggested that transition between two or more crystallographic forms of ice may occur with moisture changes and affect the K values and green compressive strength.

The reported results appear to confirm the earlier investigations by Tanasawa.

The close relationship between the K values determined for the mixtures tested and those published for ice tends to support a proposed bonding mechanism in green sand that depends upon the establishment of a silica gel, in which the water is converted to the non-stoichiometric condition.

BIBLIOGRAPHY

(3) Paschkis, V., "Studies on the Solidification of Castings," Trans. A.F.S., Vol. 53, 1945, p. 901.

(4) Paschkis, V., "Solidification of Cylinders," Trans. A.F.S., Vol. 61, 1953, p. 143.

(5) Brandt, F. A., Bishop, H. F., and Pellini, W. S., "Solidification of Various Metals in Sand and Chill Molds," Trans. A.F.S., Vol. 62, 1954, p. 646.

(6) Brandt, F. A., Bishop, H. F., and Pellini, W. S., "Solidification of Steel from Sand and Chill Walls," Trans. A.F.S., Vol. 59, 1951, p. 435.

(7) Pellini, W. S., "Practical Heat Transfer," Trans. A.F.S., Vol. 61, 1953, p. 603.

(8) Lucks, C. F., "Thermal Conductivity of Sand Mixtures," Trans. A.F.S., Vol. 56, 1948, p. 363.

(9) Adams, C. M., and Taylor, H. F., "Flow of Heat from Sand Castings by Conduction, Radiation, and Convection," Trans. A.F.S., Vol. 65, 1957, p. 170.

(10) Fitch, A. L., "A New Thermal Conductivity Apparatus," American Physics Teacher, Vol. 3, 1935, p. 135.

(11) Schuhmann, R., "Metallurgical Engineering," Addison-Wesley, 1952, p. 108.

(12) Baker, D. F., and Williams, D. C., "Factors Involved in Making a Sand Mixture, Preliminary Study No. 1," Trans. A.F.S., Vol. 61, 1953, p. 309.

(13) Paschkis, V., "Heat Flow in Moist Sand," Trans. A.F.S., Vol. 59, 1951, p. 381.

(14) Williams, D. C., "Factors Involved in Making a Sand Mixture, Preliminary Study No. 2," News in Engineering, The Ohio State University, Vol. 33, No. 2, April 1961, p. 11.

(15) Williams, D. C., op. cit.

(16) Paschkis, V., op. cit.

(17) Tanasawa, Y., "A New Method for the Measurement of the Thermal Constants of Wet Substance (2nd Report)," Trans. Soc. of Mech. Engineers (Tokyo), Vol. 1, 1935, p. 217.

A STUDY OF SOME FOUNDRY VARIABLES AFFECTING THE OCCURRENCE OF VISIBLE NONMETALLIC SURFACE DEFECTS IN STEEL CASTINGS

J. B. Caine, E. H. King, J. S. Schumacher*

SUMMARY

Evidence is presented that nonmetallic defects in steel castings are due to at least four factors: furnace slag, fluxed ladle lining material (ladle slag), reoxidation products formed during pouring (ceroxides), and possibly eroded sand.

Evidence is also presented that the cause of these defects cannot be determined by visual examination except in extreme cases. Differentiation even by chemical analysis is difficult with acid practice. Extreme slag type defects are possible when no slag like material is visible on or under the metal stream from lip pour, or tea pot, ladles. A reevaluation of steel ladle, pouring, and gating practices is indicated.

A choke in the sprue prevents most of the slag and fluxed ladle lining from entering the gate system and casting cavity. When only the sprue is choked, defects similar to those caused by slag and fluxed ladle lining still occur, but to a lesser degree. These defects are presumably due to slags or skums caused by reoxidation of the metal by the oxygen in the mold gases while it is flowing through an unfilled gate system. The term "ceroxide" is used in this report to identify these reoxidation products.

Reoxidation products formed during pouring, as well as slag and fluxed ladle lining, can be centrifuged and trapped in a side riser with a tangent gate matched to the pouring rate of the individual mold. The same effect can be obtained without centrifuging if the entire gate system is kept full during pouring.

The size of the test casting caused a flow pattern in the casting cavity that did not form more reoxidation products. Therefore, this phase of the problem cannot be discussed at present.

DISCUSSION

This is the third report of a series, reporting studies on factors influencing visible nonmetallic macroinclusions in steel castings. The first two, (1) and (2), report on miscroscopic examinations of the bonding of foundry sands by clay and of mold surfaces in contact with liquid metal. They show the possibility of erosion and agglomeration of individual sand grains by the movement of liquid metal as *one* cause of visible nonmetallic macroinclusions, especially in steel castings.

The cumbersome term, visible nonmetallic macroinclusions, is used throughout this report rather than the shorter terms "sand", "dirt", "ceroxides", and "skums" to avoid confusion. The shorter terms mean different things to different men. Visible nonmetallic macroinclusions has been selected to cover all such inclusions. It is one aim of this report to study some of the different interrelated phases that are now lumped together when the shorter terms are used by steel foundrymen.

There are at least four possible causes of visible nonmetallic macroinclusions in steel castings.

1. Furnace slag.
2. Ladle Slag. This type of slag includes bottom pour nozzle erosion as well as slag from lip and tea pot ladles. Bottom pour nozzle erosion is covered in another investigation (3) and is not considered in this report.
3. Reoxidation Products. These are another type of slag formed when liquid steel is oxidized by air and mold gases to form manganese silicate slags, or skums containing various amounts of iron oxide and alumina (4) (5) (6).
4. Displaced sand. Displacement caused by scabbing, buckling and spalling is not considered in this report. Eroded sand as discussed in reference (2) is considered in light of the steel foundry problem of visible nonmetallics in, or just below the casting surface, with no evidence of scabbing, buckling, or spalling.

A major complication is the visual similarity of the products of these four interrelated phases. Furnace slag, ladle slag, reoxidation products, form visually similar macroinclusions, the "ceroxide" and "skum" defects. Furnace slag, tea pot and lip pour ladle slag, reoxidation products formed with acid furnace, and ladle practice cannot even be differenciated chemically with certainty. Fortunately, these three phases can be differentiated chemically with basic practice, as will be discussed later. This is important, for if the cause cannot be determined the cure is difficult.

A further complication arises because these four phases, due to different causes, are mixed and very seldom occur separately. For example, every mass of nonmetallic material taken from a mold cavity before it contacts the mold wall studied to date contains angular, unfused sand grains. The liquid phase may be furnace slag, ladle slag, or reoxidation products. All seem to pick up sand grains while the mold is filled with steel. It seems impossible to solve

* Consultant, President, Vice President, respectively, Hill and Griffith Co., Cincinnati, Ohio.

the problem by eliminating one phase. At least two must be eliminated simultaneously. When the nonmetallic material contacts the mold wall it wets and penetrates the sand and is further contaminated by sand grains.

It would seem that eroded sand can be visually distinguished from the slags by its angularity in contrast to the liquid slags. This does not seem to be true in all instances. Koch (7) has reported changing the macroinclusions from the liquid ceroxide type to almost individual sand grains by adding reducing agents to the mold surface. VanVlack, Flinn and Colligan (3) have studied erosion from aluminum silicate bottom pour nozzles that at least occasionally, causes seemingly solid, angular macroinclusions (8).

A detailed study of the MnO-SiO_2-FeO-Al_2O_3 phase diagrams reveals that a slight change in chemical composition in the order of 5 percent SiO_2 or Al_2O_3, at 45 to 50 percent SiO_2, can increase melting points from under 2000 degrees F to over 2800 degrees F. This would indicate that furnace slag, ladle slag, and reoxidation products that are now considered viscous liquids can be solids at normal steel pouring temperatures due to a slight change in composition. Such a change is possible during pouring due to a number of variables: absorption of SiO_2 from sand, decrease in Al_2O_3 content due to exhaustion of the aluminum in the metal, and a decrease in MnO and FeO content. Conversely, greater fluidity is possible by other slight changes in composition.

It became apparent early in an investigation of the sand phase of macroinclusions in the Hill and Griffith laboratory that the other phases would have to be studied, evaluated and controlled. Unless this was done it would have been impossible to evaluate the test castings. This report covers this part of the general investigation.

The same test casting used by Koch (7) was used for this work. Details are given in Figure 1. The sands contained 6 percent western bentonite and ½ percent cereal. The sand properties are given in Table I. The range in properties is due to use of sands of various grain sizes. No other effect was noted with this particular test casting due to grain size variations of the sand except a slight difference in surface smoothness. This difference in surface finish would be obliterated by usual shot blasting.

TABLE I

Percent Water	3.0	-	3.9
Green Permeability	80	-	180
Green Compression Strength	8.2	-	10.6 psi
Green Shear Strength	2.6	-	3.4 psi
Weight, 2 in. Specimen	156	-	159g
Molds jolted and squeezed to	85	-	90 green hardness

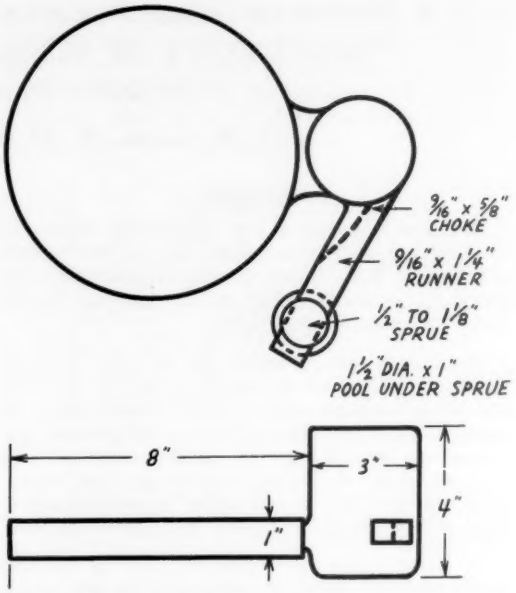

Figure 1—Details of test casting used, showing unchoked and choked runner variations.

Molds were not dried, were closed immediately, and poured within an hour with SAE type 1025 steel. The steel was melted in a 25-lb. induction furnace using a zirconia crucible. The steel was aluminum killed, except when noted otherwise, and poured directly from the furnace into the mold. Except when noted, the steel entered the mold between 2940 and 2980 degrees F. Pouring temperatures were determined with an optical pyrometer calibrated with the liquidus temperature of 1025 steel as 2780 degrees F. All heats were boiled before deoxidation.

Castings were evaluated and photographed as shaken out. None were shot blasted. The sand at the sand-metal interface glazed and fell off the flat cope and drag surfaces. The sand shown in some photographs at the riser-casting junction is adhering sand, not a scab. The surfaces of some castings show "spangles" that must not be confused with defects. "Spangling" is a surface phenomenon and is obliterated by shot blasting or heat treatment. If there is any question, the defective areas are marked on the photographs.

SLAG

As the molds were poured directly from the furnace, it acts as both the furnace and the ladle as far as slag is concerned. It was found early in the investigation that the first 6 or 8 castings poured from a new zirconia crucible gave fairly reproducible results. After these first heats the macroinclusions visible in the cope surface became larger, and incon-

Figure 2—Large, deep macroinclusions due to slag entering sprue. Note slaggy sprue and runner.

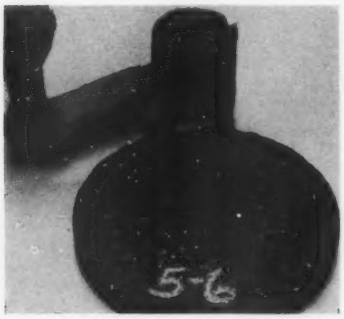

Figure 3—Normal macroinclusions from first heat from crucible. Casting represents 11 such castings.

Figure 4—Large, deep macroinclusions. No slag was seen entering sprue. Note slaggy sprue and runner.

sistent results were obtained. This was true even though all slag was removed before pouring, and no slag could be seen on the metal stream entering the sprue.

The series of test castings shown in Figures 2 - 7 were made to check the occurrence of slag by going to extremes. Casting Figure 2 was cast from a crucible that had made 20 heats, charged with rusty, wet scrap. The slag was not skimmed off and was quite visible entering the sprue. About the only surprise is the size and depth of the cope defects when compared with the normal macroinclusions of Figure 3, a casting poured from a new crucible. The casting of Figure 4 was poured from a heat following the casting of Figure 2, but the heat was skimmed thoroughly and no slag was seen entering the sprue with the metal. It was quite surprising that about the same amount of nonmetallics was present in the cope surface.

With this evidence in mind, previous castings were reviewed in relation to the number of previous melts from the crucible. It seems with the melting and pouring practice at Hill and Griffith that slag is distinguished only by the depth of the defect. This differentiation is far from certain. Figure 5 illustrates such a casting. Are the cope macroinclusions slag? It would seem so, for there is evidence of much slag on the runner surfaces. However, the casting of Figure 6 shows a perfect cope surface even though there is evidence of slag on the runner. Figure 7 illustrates an intermediate case. Are the microinclusions due to slag, or ceroxides, or a combination of the two? No certain evaluation is possible by visual examination.

This state of confusion parallels production experience, except for the degree of defects. The shape of the test casting magnifies cope defects. It was selected for this reason. The castings of Figures 2, 4, and 5 are extremes and were purposely made so. The castings of Figures 3, 6, and 7 represent production steel castings of this shape and size fairly well. Cope surfaces on shake out range from fair to perfect, with no explanation for the variation.

Many foundries use lip and teapot pouring ladles for only one heat for this reason: slag that seems invisible during pouring. However, this practice does not completely eliminate macroinclusions. It is quite possible that ladle slag and reoxidation products can both form macroinclusions that are visually indistinguishable. Excellent ladle practice may eliminate slag, but not reoxidation products. The macroinclusions of Figure 3 are probably reoxidation products. Slag is absent. Those of Figure 7 may be reoxidation products, or slag, or a combination of the two. Visual examination cannot differentiate.

Figure 5—Deep macroinclusions, probably composed of slag. Note slaggy sprue and runner.

Figure 6—Perfect cope surface, although runner shows slag.

Figure 7—Small macroinclusions may be slag, or may be ceroxides. Runner shows evidence of slag.

TABLE II

Castings	Pouring Rate	Sprue Size	Sprue Capacity (9)	Runner Size	Runner Capacity	Remarks
Figure 2 thru Figure 7	4-5 lbs/sec.	.79 sq. in.	10 lbs/sec.	.70 sq. in	7 lbs/sec.	Gate system not full
Figure 8	4-5 lbs/sec.	.79 sq. in.	10 lbs/sec.	.35 sq. in	4 lbs/sec.	Choke full

GATING - POURING

The next variable investigated was slight variations in metal flow due to gating and pouring. Figure 8 illustrates a representative casting made with a choke in the tangent gate entering the riser. All these castings showed perfect cope surfaces as far as macroinclusions are concerned. The reason seems due to gate size and pouring rate, as summarized in Table II.

The castings of Figures 2 - 7 were poured with a partially full gate system. Presumably there was not enough velocity to develop a swirl in the riser to centrifuge and trap nonmetallics in the riser. The castings of Figure 8 were poured with a full gate system because of the choke and presumably developed enough velocity to create a swirl in the riser that trapped slag and reoxidation products before they could enter the casting cavity. This is not proven by the castings themselves. Figures 9 - 11, showing mercury flowing through glass gate systems, indicate that the hypothesis has some basis on fact. These findings are also in accord with those of SFSA Research Report 31.

The gate system of Figure 8 is not unique in its ability to deliver clean metal to the casting cavity. That of Figure 12 also produces consistently clean copes at low pouring rates. Although the gates of Figures 8 and 12 may seem entirely different they have one point in common: both can be kept full with pouring rates of 5 lbs. per second, or less. Even though the gate of Figure 12 seems ridiculously small to the point of being impractical for steel, it produces sharp test castings. The velocity imparted by the gate of Figure 12 eliminates the cold shuts of Figure 8 that are due to the low velocity of the metal filling the mold cavity from a tangent gate. Velocity in this instance has been dissipated by the swirling action in the riser.

Faster pouring rates than the 2 lbs./sec. using the gate of Figure 12 have, to date, caused inconsistent results. In one production test the gate system of Figure 12, using ⅝ in. square runners and in gates delivering 5 to 6 lbs./sec., has produced clean copes. In another test a similar system, made a little larger to deliver 6 lbs./sec., caused extreme turbulence and large macroinclusions in the cope surface. The difference in metal flow seemed to be due to entering velocity of the metal from the ladle into the sprue, but this has not been proven to date.

Therefore, it must be emphasized that the discussion of the previous paragraphs, especially the exact dimensions of the gate systems, only applies to the pouring practice at the Hill and Griffith laboratory. However, the general premise that full gate systems are necessary seems basic. This general premise cannot at present be applied blindly. The exact gate system must be adapted to the individual pouring

Figure 8—Casting made with choked runner entering riser. Cope has cold shuts and is spangled, but no macroinclusions are visible. Casting represents 3 such castings.

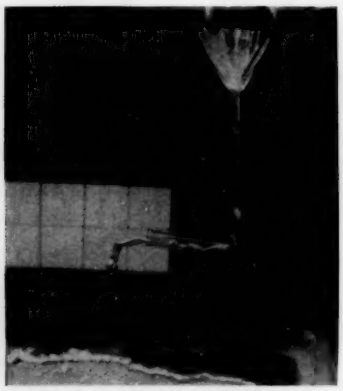

Figure 9—Sprue: runner: ingate ratio of 1:2:2. Pouring basin and sprue not full, as with normal steel foundry practice. Exit velocity equals 6 inches per second.

Figure 10—Sprue: runner: ingate ratio of 1:(.8):(.8). Pouring basin and sprue not full. Exit velocity equals 19 inches per second.

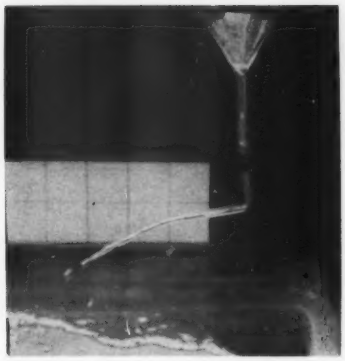

Figure 11—Sprue: runner: ingate ratio of 1:(.4):(.4). Pouring basin and sprue not full. Exit velocity equals 35 inches per second.

Figure 12—Casting poured with ¾ inch diameter sprue and ½ inch square runner and ingate. Pouring rate was 1.8 pounds per second. Cope was spangled but no macroinclusions or cold shuts were visible. Higher pouring rates produced extreme turbulence.

Figure 13—Typical casting poured with strainer core at the top of sprue. Normal macroinclusions present and cold shut due to slow pour (1.8 pounds per second) and low velocity.

practice. This is true also for the tangent gate into a slide riser. A choked runner helped under the particular conditions of these experiments. It is quite possible that a similar choke would be detrimental with other pouring conditions, especially with higher pouring rates.

A tangent gate into a side riser cannot be used on all production castings. Production experience also indicates, but does not prove, that reoxidation macroinclusions can form in the casting cavity even though clean metal entered the cavity. The choked tangent gate is therefore not satisfactory for this investigation. It is not the aim of the experiments to make good castings, rather the reverse, to make bad castings so that the factors influencing macroinclusions can be studied.

Strainer cores and small sprues were then tried in an effort to separate slag from macroinclusions due to other causes. The choke was moved from the riser to the sprue and pouring basin. Figure 13 illustrates a typical casting made with strainer cores at the top of the sprue. A drastic choke was used, decreasing the pouring rate from 4 - 5 lbs./sec. to 1.8 −2.0 lbs./sec. Even though these castings were poured with metal melted in a crucible that had made over 20 heats, all show cope defects similar to those in castings poured from a new crucible, as in Figure 3. Although the metal was skimmed thoroughly before tapping and no slag was seen on the stream entering the sprue, appreciable slag rose to the surface of the pool of metal in the pouring basin above the strainer core while pouring.

Figure 14 illustrates a casting made with a strainer core at the base of the sprue. Subject to check, it seems as if there is a significant difference due to the position of the core. The macroinclusion of Figure 14 is different from those shown previously. It is larger, shallower, and seems to be less liquid, to the point of being composed of almost solid material. It is possible that increased velocity through the strainer core eroded sand. However, checks on this point are necessary.

Figure 15 illustrates a casting made with a ½ in. diameter sprue showing normal macroinclusions. The choke of the sprues of Figures 13, 14 and 15 is about the same resulting in similar pouring rates.

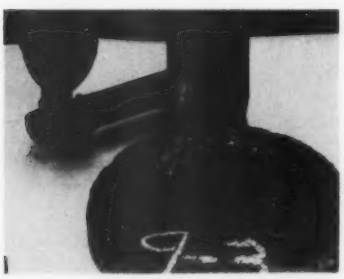

Figure 14—Casting poured with strainer core at base of sprue. Macroinclusion shown was composed of almost solid material.

Figure 15—Casting poured with ½ inch diameter sprue and large runner. Normal macroinclusions present and cold shut due to slow pour (2 pounds per second) and low velocity.

Figure 16—Casting poured at 2830 degrees F through ⅞ inch diameter sprue at a pouring rate of 5 pounds per second. No macroinclusions visible.

TABLE III

Approximate Analyses of Material Causing Cope Defects in Steel Castings

Melting Practice	Analyses of Macroinclusions (Percent) SiO_2	MnO	FeO	Al_2O_3	CaO	MgO	Possible cause of the Macroinclusion
Basic	49	20	12	11	4	6	About 80% reoxidation products, 20% slag
Basic	45	13	21	14	5	2	same
Basic	45	3	5	18	16	11	About 55% reoxidation products, 45% furnace and ladle slag
Basic	22	—	—	—	5	49	Almost all ladle slag
Used basic ladle lining	25	27	6	10	11	35	

The small sprue has also effectively separated furnace and ladle slag macroinclusions from those due to other causes. The castings illustrated in Figures 8, 13, 14 and 15 strongly indicate that macroinclusions form in the gate system, causing cope defects. They also indicate that these inclusions can be trapped in a riser if a tangent gate is used that is matched to the pouring rate. It seems that the shape of this particular casting does not cause a flow pattern that may cause additional macroinclusions in the casting cavity itself.

It may seem that the points that have just been discussed are too elementary for serious discussion. However, they are anything but simple. The complicating factor is that visual control and visual evaluation are not applicable. Present production controls are all visual. The service life of lip and teapot ladles in the steel foundry is based on visual slagging. It is definite that serious macroinclusions are possible when no slag is visible during pouring. Slagging in the tests of this report occurred after 6 to 8 heats—possibly equivalent to 6 to 8 fillings of a pouring ladle, not 6 to 8 heats poured.

Unless the gate system is drastically choked, slag, visible or invisible, can enter the casting cavity. The great majority of steel foundries pour only partially filled gate systems and are particularly vulnerable to defects due to ladle slag. Even if slag is effectively controlled there is the problem of more slag-like material forming in the gate system, or possibly even in the casting cavity. This is shown by the test castings poured with strainer cores in comparison with those poured with a choked tangent gate.

An idea of the complexity of the problem can be gained from the chemical analyses of nonmetallic macroinclusions taken from production steel castings. The macroinclusion material of Table III was taken from the surface of production castings after solidification and cooling to room temperature. Therefore, this material had contacted and permeated the sand of the sand-metal interface. The original liquid material is contaminated with additional sand grains of the mold wall. The analyses of Table III have been corrected for these contaminating sand grains. The corrections of Table III were made by calculation, estimating that 55 percent of the analyzed material was sand grains, 45 percent, the liquid that permeated these grains as the sand wall.

Although chemical analysis shows the presence of three types of slags, furnace slag, fluxed ladle lining material, and a material rich in MnO (ceroxide), the appearance of these materials on the castings on shake-out is the same. With the basic process, furnace slag can be distinguished chemically by its CaO content; ladle lining, by its MgO content. This is not possible with the acid process, using silica refractories.

TABLE IIIA

Approximate Analyses of Material Causing Cope Defects in Steel Castings

Melting Practice	Analyses of Macroinclusions (Percent) SiO_2	MnO	FeO	Al_2O_3	CaO	MgO	Possible Cause of the Marcroinclusion
Acid	53	15	9	23	—	—	Probably ladle slag
Acid	44	20	16	14	tr	tr	Unknown
Acid	67	16	5	8	0.5	1.5	Unknown
Acid	44	28	12	7	—	—	Probably reoxidation product
Used Acid Ladle Lining	66	9	6	13	—	—	

TABLE IV

Analysis of Nonmetallic Material Before Contact with Mold Wall

Sample Source	Melting Practice	Unfused Sand Grains (Percent)	Analysis of Liquid Phase Corrected for Sand Grains (Percent)					
			SiO_2	MnO	FeO	Al_2O_3	CaO	MgO
Surface of Metal in Ladle	Acid	nil	49	31	7	10	—	—
Metal in Ladle	Acid	nil	44	23	7	23	tr	1
Metal in Ladle	Basic	nil	46	39	6	6	1	9
Riser Surface	Acid	20	35	32	29	4	—	—
Riser Surface	Basic	28	48	25	11	21	tr	3
Riser Surface	Basic	37	48	38	7	6	3	2
Riser Surface	Basic	5	51	22	10	14	tr	tr

The chemical composition of reoxidation products uncontaminated by sand grains of the mold wall can be determined by collecting the slag or skum forming on the surface of liquid steel in slag free ladles, or in risers before contact with the mold wall. (See Table IV.) This sampling eliminates some, but not all, of the uncertainties of Table III. The analyses of Table III should always be questioned as to the correctness of the calculations for contaminating sand grains.

A distinguishing feature of the analyses of the reoxidation products, especially with acid practice, is the relatively high MnO contents of the reoxidation products when compared with furnace and ladle slag. However, differentiation by chemical analyses is far from sure.

All the slags, or skums of Table IV fall close to the eutectic trough of the SiO_2-MnO-FeO-Al_2O_3 system with melting points from 2085 to 2190 degrees F. The Al_2O_3 acts as a flux. When the SiO_2 content is over 45 percent, 8 to 25 percent Al_2O_3 is needed to form eutectics with melting points under 2800 to 2900 degrees F.

POURING TEMPERATURE — DEOXIDATION PRACTICE

A series of castings were poured at 2830, 2870, 2940, and 3020 degrees F. The casting poured at 2830 degrees F showed no macroinclusions visible on the surface as shown by Figure 16. The casting was not machined, so there may be macroinclusions under the surface. Cold metal tends to trap nonmetallics under the surface. The casting poured at 2870 degrees F showed a few shallow macroinclusions as shown in Figure 17. Those poured at 2940 and 3020 degrees F showed normal macroinclusions as in Figures 18 and 19. Perhaps the 3020 degrees F casting shows slightly more than normal macroinclusions, but the difference is not great.

Three castings were poured at 2940 - 2980 degrees with silicon killed steel. No aluminum was added as the final deoxidizer. None showed visible macroinclusions, but again there may be nonmetallics under the surface. The absence of aluminum may cause solid reoxidation products rather than liquid. If solid products are formed, they may be trapped under the surface easier than the liquids formed when aluminum is present.

These findings have no direct application to this investigation, nor do they have direct application in the production of small steel castings in green sand molds. However, they do explain why many foundries, especially those pouring open hearth metal, are not troubled with defects due to liquid macroinclusions. A combination of ladle slag, that should cause

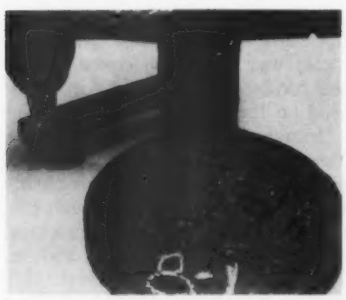

Figure 17—Casting poured at 2870 degrees F, showing smaller and shallower-than-normal inclusions and spangled surface.

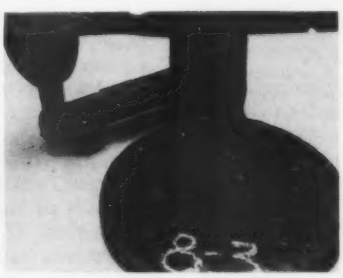

Figure 18—Casting poured at 2940 degrees F, showing normal macroinclusions.

Figure 19—Casting poured at 3020 degrees F, showing spangled surface and perhaps slightly more than normal macroinclusions.

an increase in macroinclusions during pouring of a heat, and a drop in pouring temperature, that should decrease macroinclusions due to reoxidation products, can also cause varying end results. Confusion will be compounded by visual examination since the defects formed are not visually distinguishable as to cause.

Discussion of the possible interrelation of reoxidation products and eroded sand must await further experimental work. Reference (2) showed the possibility of erosion of individual sand grains from rammed sand surfaces due to poor compaction of these surfaces. Table IV shows a significant part of nonmetallics taken from production molds while they are being filled to be unfused sand grains. This is true even though the nonmetallics are taken from the surface of the metal in the mold before they have contacted the mold wall. An investigation is now underway concerning this behavior, and a report of this study will follow in the next Journal.

REFERENCES

1. Caine, King and Schumacher, "A Microscopic Study of the Bonding of Steel Foundry Sands by Clays," *Journal of Steel Castings Research,* No. 16, January 1960.
2. Caine, King and Schumacher, "A Microscopic Study of Rammed Sand Surfaces," *Journal of Steel Castings Research,* No. 21, April 1961.
3. VanVlack, Flinn and Colligan, "Nonmetallic Macroinclusions-Causes in Steel Castings Deoxidized with Aluminum, Parts I and II," *AFS Preprints* 60 - 39, 60 - 63. *Modern Castings,* March 1960, p. 132.
4. Vingas and Caine, "Causes and Mechanics of the Skum Defect," *Foundry,* June 1959, p. 94.
5. Flinn and VanVlack, "Deoxidation Defects in Steel Castings," *AFS Transactions,* Vol. 67, pp. 295 - 299, 1959.
6. H. H. Blosjo, "Ceroxide Defect-What It is and How Its Incidence and Size can be Reduced," *Journal of Steel Castings Research,* No. 7, January 1957.
7. N. F. Koch, "A Study of the Snotter Cope Defect and Eroded Sand," *Steel Foundry Facts,* July 1956.
8. Alan Linley, Private Communication.
9. Pellini, Johnson and Bishop, "Velocities and Volume Rates of Metal Flow in Gating Systems," *AFS Trans,* Vol. 61, p. 439, 1953.
10. R. B. Snow, "Equilibrium Relationships on the Liquidus Surface in Part of the MnO-Al_2O_3-SiO_2 System," *Journal American Ceramic Society,* Vol. 26, pp. 1 - 40, 1943.

ABSTRACTS OF FUNDAMENTAL PAPERS ON STEEL CASTING RESEARCH

Based on a review of the current literature on technical research subjects. (Copies of these articles available from original publishers only.)

Melting and Refining

Dunn, Jr., E. J., "Rapid Desulfurization to 0.002 Percent Sulfur," MODERN CASTINGS, June 1961. The development of a simple desulfurization procedure that rapidly and consistently reduces sulfur from initial values as high as 0.024 percent to final residuals of 0.002 - 0.003 percent is presented. Ca was introduced into the bath as CaMnSi alloy by immersion with a plunger.

Deoxidation

Danner, G. E., and Dyble, E., "Deoxidizing Steels By Vacuum," METAL PROGRESS, May 1961. When unkilled steel is stream degassed in a vacuum, included oxygen will unite with the carbon in the steel, and boil off as carbon monoxide. Extensive tests show that steel deoxidized in this manner (rather than with metallic deoxidizers such as silicon and aluminum) will contain less gases and fewer inclusions. Properties are comparable to those of vacuum degassed steels. Sulfur inclusions are smaller and more finely dispersed and most heats contain less than 1 ppm of hydrogen.

Weldment Properties

Beachum, E. P., Johnson, H. H., and Stout, R. D., "Hydrogen and Delayed Cracking in Steel Weldments," WELDING RESEARCH SUPPLEMENT, April 1961. Investigation was centered on the combined effects of hydrogen and stress on delayed cracking in steel welds of several common compositions, both carbon and alloy. The primary tool was the Lehigh restraint test. The inert-gas consumable-electrode welding process was used with hydrogen introduced in free and combined forms. Cracking time was found to depend on the base plate and welding wire composition, restraint, and hydrogen; but the relations among these variables are complex. Cracking time was observed to lengthen at low aging temperatures, which suggests strongly that hydrogen diffusion is an important aspect of the delayed cracking mechanism. It is concluded: (a) hydrogen and restraint can cause weldment delayed cracking, (b) susceptibility is greater for the high strength base plates and weld metals, (c) residual hydrogen content does not correspond closely with welding gas composition.

INDEX—ISSUES 1-23

Key to index—Number before colon = Journal No.; Number after colon = Page No.

(Journal No.):(Page No.)

Abrasive Cleaning 3:13, 16:14

Alloys
effect of:
calcium 7:5-6
chromium 13:16
manganese 8:4, 8:11
P and S 4:15, 6:15, 18:11
selenium 14:13
silicon 8:11

Bentonite
chemical properties 8:4-6
effect on properties 12:15, 15:12, 16:1, 18:6
physical properties 8:5, 22:19

Binders—see also Bentonite
clay (incl. bentonite) 4:13, 12:14, 15:12, 16:1, 18:6-7, 22:19
inorganic 15:15, 19:14
organic 11:10-12, 12:8, 13:11, 14:12, 15:13-15, 18:5-10, 18:12

Carbon Content
effect of 3:15, 4:14, 7:9, 7:13 8:11, 14:5, 14:8, 19:6

Cast-Weld Construction 2:16, 14:7

Ceroxide Defect
composition 7:2, 14:10, 23:8-13
prevention 13:15, 23:7-13
source 7:1, 13:15, 23:7-13

Chemical Cleaning of Castings 19:10

Chills
effect on properties 17:3, 17:5-6
on ribs and bosses 3:2, 9:8
use of 3:1, 9:6

Chromium Cast Steel
13 percent Cr 13:16

Cores
gas evolution 18:8, 18:13
oil bonded 14:12, 18:6-9

Corrosion
cast steel 8:1

CO
in steel 2:13, 15:9

CO_2
in steel 2:13, 15:9

CO_2 Process—see Sodium Silicate Bonding

CO_2 Shielded Welding—see Welding

Deoxidation
aluminum 5:11, 9:13, 10:7, 14:9, 15:10, 20:1
calcium 7:5, 20:1-6, 20:7
effect on properties 7:7, 9:13, 10:1, 20:2-4, 23:13

(Journal No.):(Page No.)

graphidox 20:1
manganese 10:7
silicon 15:10
titanium 9:13, 10:8

Design
to reduce stress concentration ... 2:16, 4:8, 12:10, 15:1-4

Electro-Slag
feeding 18:1-4

Fatigue Properties 3:15, 14:4
of castings vs. weldments 4:9, 4:12

Forsterite—see Olivine

Grain Refinement
by inoculation 22:14
by vibration 10:16, 16:7
effect on properties 22:16

Hardenability 4:1-4

High Temperature
properties 7:12

Hot Tearing Tendency
influence of:
carbon content 4:14, 8:11, 19:6
design 6:7-10, 19:4, 19:10, 22:18
manganese 8:11
pouring temperature 19:6
P and S 4:15, 8:11
sand properties 7:4, 19:3
silicon 8:11

Hydrogen
in steel 2:7, 2:13, 10:5, 13:1-5, 14:13-14, 15:9-10

Inclusions 13:13
effect of:
aluminum 7:8, 10:7, 20:2, 20:6
calcium 7:6, 20:2
manganese 10:7
types 10:5

Inert Gas
flushing 13:3
melting 11:8, 13:3

Intergranular Fracture 5:10, 5:13, 9:11

Low Alloy Steels
effect of heat treatment 1:14, 3:10, 4:1-2, 8:9-10
properties 1:13, 2:8, 3:8, 3:10, 6:15, 7:12

(Journal No.):(Page No.)

Low Temperature Properties
- carbon steels ... 7:9
- low alloy steels ... 8:8
- medium alloy steels ... 8:8

Machinability ... 14:6

Magnetic
- properties of steels ... 20:10-14, 21:9-12, 21:12-15

Medium Alloy Steels
- effect of heat treatment ... 8:9-10
- properties ... 17:3-4

Melting
- basic electric ... 8:12, 18:11

Metal Penetration
- effect of:
  - pressure ... 2:11, 2:15
  - pouring temperature ... 2:12
  - sand density ... 2:11, 2:12, 2:15
- testing sand for ... 2:14

Mold-Metal Reactions—
- see also Porosity, Pinhole ... 4:15, 10:10-11, 11:3, 14:14, 15:11

Molding Materials
- effect on solidification ... 17:5

Nitrogen
- in steel ... 2:13, 5:10-12, 9:11-13, 13:1-3, 15:9-10

Olivine (Forsterite)
- for molding ... 9:9, 11:1, 17:5

Oxygen
- in steel ... 10:5, 13:3
- use in refining ... 12:1-6, 15:5-8

Permanent Molding ... 10:13

Porosity in Castings
- internal ... 10:5, 15:9, 17:2-4
- pinhole ... 10:5, 14:14

Properties—see also Alloys
- alloy ... 1:13, 2:8, 3:8-10, 6:15, 7:12, 8:8, 17:3-4
- cast vs. wrought ... 14:4
- cast-weld ... 2:16
- chemical ... 8:1
- effect of:
  - chills ... 17:3-6
  - grain size ... 22:16
  - H, N, O, etc.—see H, N, O,
  - heat treatment ... 1:14, 3:10, 4:1-2, 8:9-10
  - inclusions ... 7:7, 9:13, 10:1, 20:2-4
  - vacuum treatment—see vacuum
- fatigue ... 3:15, 4:9, 4:12, 14:4
- high temperature ... 7:12
- low temperature ... 7:9, 8:8-10
- magnetic ... 20:10-14, 21:9-12, 21:12-15

(Journal No.):(Page No.)

Risers
- calculations ... 1:2, 2:1, 3:3, 6:11, 14:10
- feeding distances ... 6:13, 18:1
- pressurized ... 9:14, 17:14

Sand
- burn-on ... 10:8
- compaction ... 3:11, 4:13, 21:1, 23:1
- evaluation test block ... 4:6, 5:1
- expansion ... 12:8
- penetration by steel—
  - see also Metal Penetration ... 2:11, 2:14
- reclamation ... 12:14
- thermal conductivity ... 23:1-6

Sand Properties ... 5:3-5, 12:6, 12:14, 15:11, 21:2-8
- effect of
  - moisture ... 23:3-6
  - re-use ... 5:5-6
  - sieve analysis ... 3:11, 3:12
  - temperature ... 9:1-5, 15:10, 21:2, 21:5, 23:2-4
- effect on:
  - hot tearing ... 7:4
  - solidification ... 17:10

Segregation in Castings ... 14:15

Shell Molding ... 3:13, 6:1, 9:9, 11:1-3
- patterns ... 6:4

Shrinkage Defects ... 12:11

Slag
- effect of FeO content of ... 8:16
- practice ... 8:14-16

Sodium Silicate Bonding ... 1:10, 5:7, 12:12
- for cores ... 5:9, 6:16
- for molds ... 5:8, 6:16, 12:13, 15:15

Solidification ... 16:9, 17:5

Statistical Analysis of Data ... 20:1, 22:1

Stress Concentration (see Design)

Surface Finish ... 14:3

Tolerances, Casting ... 13:6, 14:1

Transformation (S) Curves ... 4:1, 4:2

Vacuum
- casting ... 2:13
- degassing ... 2:7, 11:8, 12:9, 13:3
- melting ... 11:4-7
- pouring ... 2:13, 11:9

Welding
- CO_2 Shielded ... 7:15-16
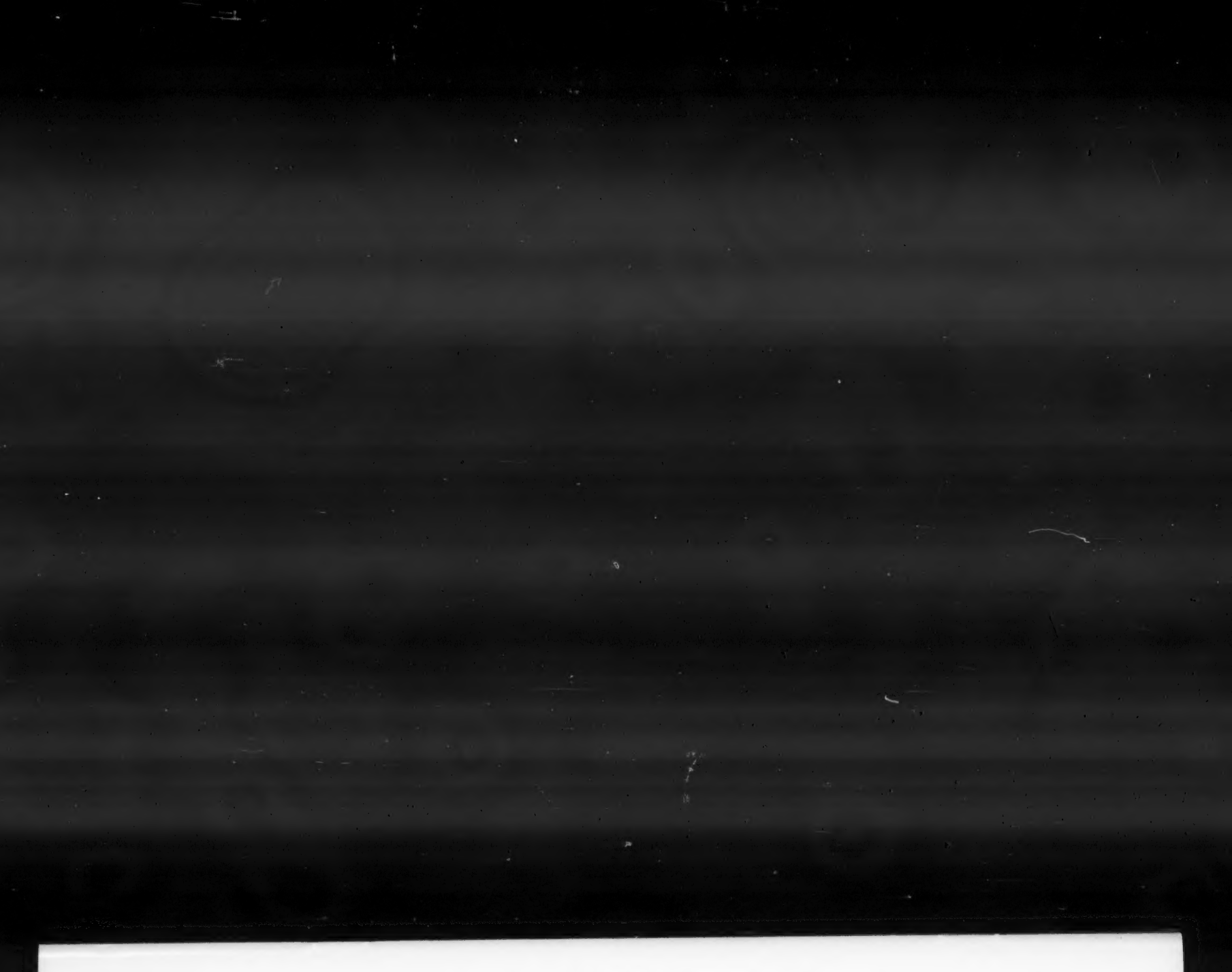
Weldments
- cracking of ... 7:12
- stress analysis of ... 4:9